



Contents lists available at ScienceDirect

Energy

journal homepage: [www.elsevier.com/locate/energy](http://www.elsevier.com/locate/energy)

# Exergetic performance evaluation and parametric studies of solar air heater

M.K. Gupta\*, S.C. Kaushik

Centre for Energy Studies, Indian Institute of Technology, Delhi 110016, India

## ARTICLE INFO

### Article history:

Received 28 January 2008

### Keywords:

Energy and exergy output  
Solar air heater  
Optimum mass flow rate  
Aspect ratio  
Duct depth

## ABSTRACT

The present study aims to establish the optimal performance parameters for the maximum exergy delivery during the collection of solar energy in a flat-plate solar air heater. The procedure to determine optimum aspect ratio (length to width ratio of the absorber plate) and optimum duct depth (the distance between the absorber and the bottom plates) for maximum exergy delivery has been developed. It is known that heat energy gain and blower work increase monotonically with mass flow rate, while the temperature of air decreases; therefore, it is desirable to incorporate the quality of heat energy collected and the blower work. First it is proved analytically that the optimum exergy output, neglecting blower work, and the corresponding mass flow rate depend on the inlet temperature of air. The energy and exergy output rates of the solar air heater were evaluated for various values of collector aspect ratio ( $AR$ ) of the collector, mass flow rate per unit area of the collector plate ( $G$ ) and solar air heater duct depth ( $H$ ). Results have been presented to discuss the effects of  $G$ ,  $AR$  and  $H$  on the energy and exergy output rates of the solar air heater. The energy output rate increases with  $G$  and  $AR$ , and decreases with  $H$  and the inlet temperature of air. The exergy-based evaluation criterion shows that performance is not a monotonically increasing function of  $G$  and  $AR$ , and a decreasing function of  $H$  and inlet temperature of air. Based on the exergy output rate, it is found that there must be an optimum inlet temperature of air and a corresponding optimum  $G$  for any value of  $AR$  and  $H$ . For values of  $G$  lesser than optimal corresponding to inlet temperature of air equals to ambient, higher exergy output rate is achieved for the low value of duct depth and high  $AR$  in the range of parameters investigated. If  $G$  is high, for an application requiring less temperature increase, then either low  $AR$  or high  $H$  would give higher exergy output rate.

© 2008 Elsevier Ltd. All rights reserved.

## 1. Introduction

Solar energy in the form of heat can be collected by using a flat-plate collector or a concentrating collector. The flat-plate collector is simple in construction, utilizes the beam as well as diffused radiation and does not require tracking. Solar air heater (SAH), because of its simplicity, is cheap and is a widely used flat-plate collector. The main applications of a solar air heater are space heating and drying for industrial and agriculture purposes. The energy collection efficiency of solar air heaters has been found to be generally poor because of their inherently low heat-transfer capability between the absorber plate and the air flowing in the duct due to unfavorable thermo physical properties of air. However, the use of air as a heat-transfer medium instead of water in solar collectors reduces the risks of corrosion, leakage and freezing, and helps to reduce weight and costs of collectors. There are various configuration parameters e.g. number of glass

cover, emissivity of absorber plate, collector length, collector duct depth or distance between absorber and bottom plates in conventional SAH, and the ratio of collector length to collector width i.e. collector aspect ratio, etc., affecting the SAH efficiency. The collector aspect ratio is the most important parameter in the design of any type of solar air heater. Increasing the collector aspect ratio for the same mass flow rate of air per unit surface area of the absorber plate increases the air velocity through the duct, which results in more heat transfer to the flowing air as well as pressure drop or required power consumption of the pump/blower. The low density and low specific heat of air combined with low heat-transfer coefficient also requires high-volume flow rates that may lead to high friction losses. The design of the flow duct and heat-transfer surfaces of solar air heaters should therefore be executed with the objectives of high heat-transfer rates and low friction losses. Yeh and Lin [1] investigated theoretically as well as experimentally the effect of collector aspect ratio on the energy collection efficiency of flat-plate solar air heaters for a constant collector area and different flow rates. They found that energy collection efficiency increases with mass flow rate and collector aspect ratio, and theoretical predictions agree reasonably well with the experimental results. Yeh and Lin

\* Corresponding author. Tel.: +91 11 26591253; fax: +91 11 26862037.

E-mail addresses: [mk\\_gupta70@rediffmail.com](mailto:mk_gupta70@rediffmail.com) (M.K. Gupta), [kaushik@ces.iitd.ac.in](mailto:kaushik@ces.iitd.ac.in) (S.C. Kaushik).

**Nomenclature**

$A_c$	collector area (m <sup>2</sup> )
$AR$	collector aspect ratio
$C_p$	specific heat (J/kg K)
$d_e$	equivalent diameter of duct (m)
$Ex$	exergy (W)
$Ex_u$	exergy output rate ignoring pressure drop (W)
$Ex_{u,p}$	exergy output rate considering pressure drop (W)
$F$	collector efficiency factor
$F_r$	collector heat removal factor
$f$	friction factor
$G$	mass flow rate per unit collector area (kg/s m <sup>2</sup> )
$h$	enthalpy (J/kg), heat-transfer coefficient (W/m <sup>2</sup> K)
$H$	solar heater duct depth (m)
$I$	radiation intensity (W/m <sup>2</sup> )
$IR$	irreversibility (W)
$k$	thermal conductivity (W/m K)
$L$	collector dimension, spacing between covers (m)
$m$	mass flow rate (kg/s)
$M$	number of glass covers
$Nu$	Nusselt number
$p$	pressure (N/m <sup>2</sup> )
$Pr$	Prandtl's number
$Q$	heat (W)
$Re$	Reynold's number
$S$	absorbed flux (W/m <sup>2</sup> )
$S_g$	entropy created due to heating of air and pressure drop (W/K)
$T$	temperature (K)
$U$	heat loss coefficient (W/m <sup>2</sup> K)
$V$	velocity (m/s)
$W_p$	pump work (W)

*Greek symbols*

$\alpha$	absorptivity
$\tau$	Transmissivity
$\beta$	tilt angle of the surface
$\tau\alpha$	transmissivity–absorptivity product
$\delta$	thickness of insulation
$\Delta p$	pressure drop (N/m <sup>2</sup> )
$\rho$	density of fluid (kg/m <sup>3</sup> )
$\mu$	viscosity of fluid (Ns/m <sup>2</sup> )
$\eta$	efficiency
$\sigma$	Stefan's constant
$\varepsilon$	emissivity

*Subscripts/superscripts*

$a$	ambient
$b$	back/bottom
$c$	collector/plate, convection
$f$	fluid
$g$	glass cover
$i$	inner, inlet, insulation
$l$	lost, overall loss
$m$	mean
$o$	outer, outlet/exit
$p$	plate
$r$	radiation
$s$	side
$S$	Sun
$st$	stagnation
$t$	top
$T$	tilted surface
$u$	useful
$w$	wind
$\infty$	wind
1, 2, 3	length, width, depth of collector

[2] investigated the effect of parallel barriers on the energy collection efficiency of flat-plate solar air heaters. The barriers divide the air channel into parallel sub-channels or sub-collectors connected in series, and air flows through them in sequentially reversed directions. Thus the effect of increasing the number of parallel barriers is equivalent to increasing the collector aspect ratio. Yeh and Lin [3] showed that the energy collection efficiency of a solar air heater can be improved by operating several sub-collectors with identical aspect ratios in place of a single collector with the same total area. They illustrated for two sub-collectors that for a constant total collector area, the energy collection efficiency increases and reaches maximum as the two sub-collectors approach the same area. They also concluded that the improvement in energy collection efficiency using sub-collectors in series increases with increase in insolation and decrease in mass flow rate. The effect of parallel barriers or using the various sub-collectors in series is to increase the velocity of flow as well as heat transfer from absorber surface to flowing air; thus the energy collection efficiency increases. It can be shown that the useful energy gain and pressure drop are strong functions of duct parameters and air flow rate per unit area of plate. As enhancement in heat transfer is accompanied by increased pressure drop of flowing air, it is desirable to incorporate the pressure drop in analysis. The analytical thermo-hydraulic performance evaluation of a solar air heater, based on equal pumping power of the collector arrays or sub-collectors arranged

in series or parallel mode, has been carried out by Karwa et al. [4]. They varied the duct depth to satisfy the condition of equal pumping power for evaluating the energy efficiency of the series or parallel arrangement of sub-collector modules, and deduced that the configuration with  $n$ -sub-collectors in parallel is to be the best for the range of parameters investigated. It is to be noted here that  $n$ -sub-collectors in series form the high AR collector.

The second law of thermodynamics-based exergy analysis is more suitable to incorporate the quality of useful energy output, and friction losses. The exergy concept based on the second law of thermodynamics provides an analytic framework for system performance evaluation. Exergy is the maximum work potential that can be obtained from a form of energy [5,6]. Exergy analysis is a useful method to complement, not to replace, the energy analysis. Exergy analysis yields useful results because it deals with irreversibility minimization or maximum exergy delivery. Exergy analysis has proven to be a powerful tool in the thermodynamic analysis of energy systems [7,8]. Lior et al. [8] presented the exergy/entropy production field equations to analyze the space- and time-dependent exergy and irreversibility fields in processes, and applied these to flow desiccation, combustion of oil droplets, and combustion of pulverized coal. The popularity of the exergy analysis method has grown consequently and is still growing [9–11]. Lior and Zhang [11] attempted to clarify the definitions and use of energy- and exergy-based performance criteria, and of the second law efficiency, to

advance the international standardization of these important concepts. In general, more meaningful efficiency is evaluated with exergy analysis rather than energy analysis, since exergy efficiency is always a measure of the approach to the ideal. Howell and Bannerot [12] analyzed solar collector performance in terms of optimum outlet temperature, which maximizes the work output of ideal heat engine cycles utilizing the collector heat output. This work output from the useful heat of a solar collector is equal to the exergy output of the collector for infinite mass flow rate of working fluid, ignoring the pressure drop in the collector.

Bejan [13,14] carried out the exergetic analysis without considering frictional pressure drop and using simplified models for a number of simple solar collector systems. For isothermal collectors, he deduced that optimum temperature by neglecting the internal thermal conductance of the collector is the geometric mean of stagnation and ambient temperature; otherwise it is in between the geometric mean of stagnation and ambient temperature, and the stagnation temperature. The stagnation temperature is the maximum temperature attained by the solar collector when there is no flow of working fluid through the solar collector or when useful heat gain is zero. For non-isothermal collectors or practical collectors, he concluded that the collector fluid must be circulated at a higher rate through collectors with high heat loss or having low stagnation temperature. He also pointed out that irreversibility in the collector varies with mass flow rate and the mass flow rate must be optimum for minimum entropy generation. Manfrida [15] pointed out that to obtain higher exergetic or rational efficiency, the difference between the collector inlet and outlet temperatures should be small for low-performance collectors and higher for selective-coated, evacuated or focusing collectors. Kar [16] proved that for maximum exergy output for the flat-plate solar collector for a particular mass flow rate, there is an optimum inlet temperature. Suzuki [17] discussed about the various terms like exergy inflows, exergy leakage and exergy annihilation (destruction) related to the general theory of exergy balance, and applied these to flat-plate and evacuated solar collectors. He evaluated the effect of heat capacity on various exergy loss terms and exergy gain by the working fluid. Altfeld et al. [18] discussed the basic concepts regarding the exergy analysis of the solar air heater, considering the compression energy needed to overcome pressure drop. They evaluated the various losses during the collection of solar energy and represented in the form of energy and exergy flow diagrams. They considered the net exergy flow as a suitable quantity for balancing the useful energy and friction losses, and for the optimum design of absorber and flow ducts. They also determined an optimum flow velocity for maximizing the net exergy gain. The second law optimization of different absorber models for constant ambient temperature and global radiation, and for fixed high mass flow rates were carried out by Altfeld et al. [19]. However, the analysis given therein is implicit and not easy to follow, and could not be further used for other systems. The geometry of rib roughness considered by them is not suitable for frictional power

consideration as it is unnecessary to use ribs on the bottom plate for a solar air heater. Torres-Reyes et al. [20] followed the non-isothermal model given by Bejan [14] and presented the procedure to establish the optimal performance parameters for minimum entropy generation during the collection of solar energy. They evaluated stagnation temperature, mass flow number, minimum entropy generation number and the optimal mass flow rate of the working fluid and applied the developed procedure to a typical solar drier. Luminosu and Fara [21] carried out the exergy analysis-based numerical simulation by expressing the exergy efficiency as a function of mass flow rate and collector area; they obtained the optimum area by taking the inlet temperature equal to ambient temperature and assuming a constant value of the overall loss coefficient. They determined the local optimum mass flow rate for each area of the collector from a range of considered flow rates; and for the area ranging from 0 to 10 m<sup>2</sup> and for a mass flow rate from 0 to 0.0076 kg/s, they evaluated the global optimum mass flow rate and area. It may be noted here that the expression for heat gain or exergy output of the collector is a function of mass flow rate per unit area. They also analyzed the influence of the heat loss coefficient, glass quality, solar flux density and specific heat of fluid on the flat solar collector exergy, heat gain, exergy efficiency and temperature rise of the fluid through the collector.

The analyzed relevant literatures contain studies on the dependences of the exergy output on fluid mass flow rate and temperature of fluid at inlet to the collector. It has been recommended [1–3] to use high AR and mass flow rate on the basis of energy analysis; thus the aim of the present investigation is, to determine the effect of G, AR, and H on energy as well as on exergy output rate.

## 2. Theoretical analysis

### 2.1. Analysis of solar air heater

The collector under consideration consists of a flat glass cover and a flat absorber plate with a well insulated parallel bottom plate, forming a passage of high duct aspect ratio (the ratio of collector width to collector duct depth) through which the air to be heated flows as shown in Fig. 1. The heat gain by air may be calculated by the following equations:

$$Q_u = A_c[S - U_l(T_{pm} - T_a)] = A_c[\tau_g \alpha_p I_T - U_l(T_{pm} - T_a)] \quad (1)$$

$$Q_u = mc_p(T_o - T_i) \quad (2)$$

$$Q_u = A_c F_r [S - U_l(T_i - T_a)] \quad (3)$$

where  $F_r$  is collector heat removal factor and is given by

$$F_r = \frac{mc_p}{U_l A_c} [1 - e^{-(U_l A_c F)/mc_p}] \quad (4)$$

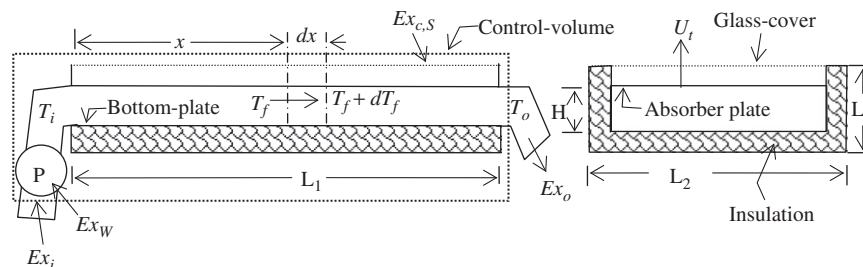


Fig. 1. Flat-plate solar air heater.

The collector efficiency factor  $F'$  is

$$F' = \left(1 + \frac{U_l}{h_e}\right)^{-1} \quad (5)$$

and the equivalent heat-transfer coefficient  $h_e$  is

$$h_e = h_{c,f-p} + \frac{h_{r,p-b}h_{c,f-b}}{(h_{r,p-b} + h_{c,f-b})} \quad (6)$$

The mean absorber plate temperature from Eqs. (1) and (3) is given by

$$T_{pm} = T_a + \frac{Q_l}{U_l A_c} = T_i + \frac{Q_u}{A_c F_r U_l} (1 - F_r) \quad \text{where} \quad (7)$$

$$Q_l = S A_c - Q_u$$

The mean fluid temperature ( $T_m$ ), is given by

$$T_m = \frac{1}{L_1} \int_0^{L_1} T_f dx = T_i + \frac{Q_u}{A_c F_r U_l} \left(1 - \frac{F_r}{F'}\right) \quad (8)$$

### 2.2. Heat transfer and pressure drop

The overall heat loss coefficient  $U_l$  is the sum of  $U_b$ ,  $U_s$  and  $U_t$ , of which  $U_b$  and  $U_s$  for a particular collector can be regarded as constant while  $U_t$  varies with temperature of the absorber plate, number of glass covers and other parameters. The top heat loss coefficient  $U_t$  is evaluated empirically [22] by

$$U_t = \left[ \frac{M}{(C/T_{pm})[(T_{pm} - T_a)/(M + f')]^{0.252} + \frac{1}{h_w}} \right]^{-1} + \left[ \frac{\sigma(T_{pm}^2 + T_a^2)(T_{pm} + T_a)}{[1/(\varepsilon_p + 0.0425M(1 - \varepsilon_p))] + [(2M + f' - 1)/\varepsilon_c] - M} \right] \quad (9)$$

in which  $f' = [(9/h_w) - (9/h_w^2)](T_a/316.9)(1 + .091M)$ ,  $C = 204.429(\cos \beta)^{0.252}/L^{0.24}$  and the heat-transfer coefficient at the top of the cover due to wind is

$$h_{c,c-a} = h_w = 5.7 + 3.8V_\infty \quad (10)$$

The overall heat loss coefficient is given by

$$U_l = U_b + U_s + U_t$$

in which

$$U_b = \frac{k_i}{\delta_b} \quad \text{and} \quad U_s = \frac{(L_1 + L_2)L_3 k_i}{L_1 L_2 \delta_s} \quad (11)$$

The radiation heat-transfer coefficient  $h_{r,p-b}$  between the absorber plate and the bottom plate is given by

$$h_{r,p-b}(T_{pm} - T_{bm}) = \frac{\sigma(T_{pm}^4 - T_{bm}^4)}{[(1/\varepsilon_p) + (1/\varepsilon_b) - 1]} \quad (12)$$

For small temperature difference between  $T_{pm}$  and  $T_{bm}$  on the absolute scale, the above equation can be written as

$$h_{r,p-b} \cong \frac{4\sigma T_{av}^3}{[(1/\varepsilon_p) + (1/\varepsilon_b) - 1]}$$

where  $T_{av} = (T_{pm} + T_{bm})/2$  and  $T_{av}$  is taken equal to  $T_m$  in iterative calculation using the same logic.

For smooth duct the convection heat-transfer coefficients between, flowing air and absorber plate  $h_{c,f-p}$ , and flowing air and bottom plate  $h_{c,f-b}$  are assumed equal. The following correlation for air, for fully developed turbulent flow (if the length to equivalent diameter ratio exceeds 30) with one side heated and the other side insulated [23], is appropriate:

$$Nu = \frac{h_{c,f-p} d_e}{k_a} = 0.0158(Re)^{0.8} \quad (13a)$$

If the flow is laminar, then following correlation by Mercer [24] for the case of parallel smooth plates with constant temperature on one plate and the other plate insulated is appropriate:

$$Nu = \frac{h_{c,f-p} d_e}{k_a} = 4.9 + \frac{0.0606[Re Pr (d_e/L_1)^{0.5}]}{1 + 0.0909[Re Pr (d_e/L_1)^{0.7}](Pr)^{0.17}} \quad (13b)$$

The characteristic dimension or equivalent diameter of duct is given by

$$d_e = \frac{2L_2 H}{(L_2 + H)} \quad (14)$$

The Reynolds number  $Re$  is calculated by

$$Re = \frac{\rho V d_e}{\mu} = \frac{\rho m}{\mu L_2 H \rho} \frac{2L_2 H}{(L_2 + H)} = \frac{2m}{\mu(L_2 + H)} \quad (15)$$

The pressure loss  $\Delta p$  through the air heater duct, is

$$\Delta p = \frac{4f L_1 V^2 \rho}{2d_e} \quad (16)$$

If  $Re = (\rho V d_e / \mu) \leq 2300$ , i.e. laminar flow, then the coefficient of friction is calculated by

$$f = \frac{16}{Re} \quad (17a)$$

otherwise the coefficient of friction  $f$  for the turbulent flow in a smooth air duct is calculated from the Blasius equation, which is

$$f = 0.0791(Re)^{-0.25} \quad (17b)$$

### 2.3. Energy and exergy output rate

The useful energy or heat gain by air is given by

$$Q_u = A_c F_r [S - U_l(T_i - T_a)] = m c_p (T_o - T_i) = A_c [\tau_g \alpha_p I_T - U_l(T_{pm} - T_a)]$$

The law of exergy balance [5,6], considering SAH (Fig. 1) as a control volume (CV), can be written as

$$Ex_i + Ex_{c,s} + Ex_W = Ex_o + IR \quad (18)$$

where  $Ex_i$  and  $Ex_o$  are the exergy associated with the mass flow of air entering and leaving the CV;  $Ex_{c,s}$  is the exergy of solar radiation falling on glass cover;  $Ex_W$  is the exergy of work input required to pump the air through SAH, and  $IR$  is irreversibility or exergy loss of the air heating process.

The heat flux is received from the sun and collected by air flowing through the solar air heater. The irreversibility occurs at various stages like: flux falling on the transparent cover, absorption by the absorber surface and heat loss to ambient. The useful exergy gain  $Ex_{u,p}$ , considering pressure drop or blower work, by air is calculated by

$$Ex_{u,p} = Ex_o - Ex_i - Ex_W = m c_p \left[ (T_o - T_i) - T_a \ln \frac{T_o}{T_i} \right] - \frac{T_a}{T_i} W_p \quad (19)$$

The  $[m c_p \ln(T_o/T_i) + (W_p/T_i)] = S_g$  is the sum of entropy created due to the heating of air and pressure drop or pump/blower work.

The pump (blower) work  $W_p$  is calculated by

$$W_p = \frac{m \Delta p}{(\eta_{pm} \rho)} \quad (20)$$

The pump-motor efficiency  $\eta_{pm}$  is considered equal to 0.85.

**Table 1**  
Properties of air

$T$ (°C)	$\rho$ (kg/m <sup>3</sup> )	$C_p$ (KJ/kg K)	$\mu \times 10^6$ (N s/m <sup>2</sup> )	$k$ (W/m K)	(Pr)
0	1.293	1.005	17.2	0.0244	0.707
10	1.247	1.005	17.7	0.0251	0.705
20	1.205	1.005	18.1	0.0259	0.703
30	1.165	1.005	18.6	0.0267	0.701
40	1.128	1.005	19.1	0.0276	0.699
50	1.093	1.005	19.6	0.0283	0.698
60	1.06	1.005	20.1	0.029	0.696
70	1.029	1.009	20.6	0.0297	0.694
80	1	1.009	21.1	0.0305	0.692
90	0.972	1.009	21.5	0.0313	0.69
100	0.946	1.009	21.9	0.0321	0.688
120	0.898	1.009	22.9	0.0334	0.686
140	0.854	1.013	23.7	0.0349	0.684

2.4. Optimum mass flow rate for maximum exergy output rate ignoring pump work

The exergy output rate (Eq. (19)) besides pump work also depends on the useful heat gain, inlet temperature of air and temperature increase of air. Thus there should be an optimum flow rate for a given inlet temperature of air and ambient condition. At no-flow condition the quantity and quality of heat energy collected are zero, while at infinite flow rate coupled with near-ambient inlet temperature of air, the quality (exergy) of heat energy collected reduces. If the Bliss equation is used for the collector then

$$Q_u = A_c F' \left\{ S - U_l \left[ \frac{(T_i + T_o)}{2} - T_a \right] \right\} = m c_p (T_o - T_i) \quad (21)$$

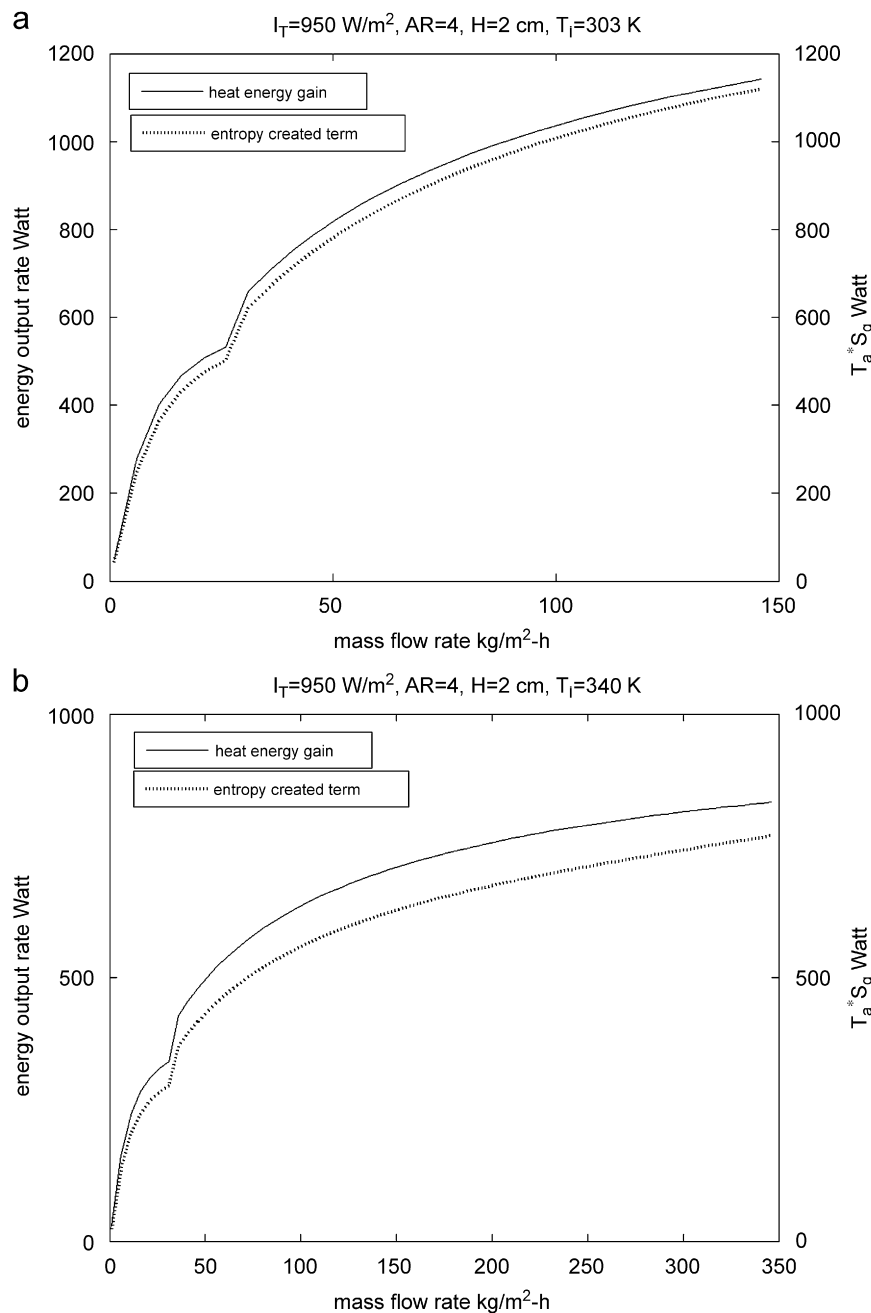


Fig. 2. Variation of useful heat gain and  $T_a \times S_g$  for a fixed value of solar radiation intensity for (a) low and (b) high inlet temperature of air.

Writing,  $\log(T_o/T_i) \cong (2(T_o - T_i))/(T_o + T_i)$ , as  $T_o/T_i \leq 2$  (for SAH), in the exergy output equation (19) by ignoring pressure drop, then the  $Ex_u$ , exergy output, ignoring pressure drop is

$$Ex_u = Q_u - mc_p T_a \frac{2(T_o - T_i)}{(T_o + T_i)} = Q_u \left[ 1 - \frac{2T_a}{(T_o + T_i)} \right]$$

$$Ex_u = A_c F' \left\{ S - U_l \left[ \frac{(T_i + T_o)}{2} - T_a \right] \right\} \left[ 1 - \frac{2T_a}{(T_o + T_i)} \right] \quad (22)$$

For maximum exergy output differentiating  $Ex_u$  w.r.t  $(T_o + T_i)/2$  and substituting equal to zero we get

$$\left( \frac{T_o + T_i}{2} \right)^2 = T_a \left( T_a + \frac{S}{U_l} \right) \Rightarrow (T_o + T_i)_{opt} = 2\sqrt{T_a T_{st}}$$

where  $[T_a + (S/U_l)] = T_{st}$  is the stagnation temperature.

Substituting  $(T_o + T_i)_{opt}$  in Eq. (21) and solving for  $m$  we get

$$m_{opt} = A_c F' \{ S - U_l [\sqrt{T_a T_{st}} - T_a] \} / 2c_p (\sqrt{T_a T_{st}} - T_i)$$

Putting  $S = U_l(T_{st} - T_a)$  we get

$$m_{opt} = A_c F' U_l (T_{st} - \sqrt{T_a T_{st}}) / 2c_p (\sqrt{T_a T_{st}} - T_i)$$

• Case I: if  $T_i = T_a$  then

$$m_{opt} = A_c F' U_l (T_{st} - \sqrt{T_a T_{st}}) / 2c_p (\sqrt{T_a T_{st}} - T_a) = A_c F' U_l \sqrt{T_{st}} / 2c_p \sqrt{T_a}$$

From the above relation we can say that  $m$  must be finite.

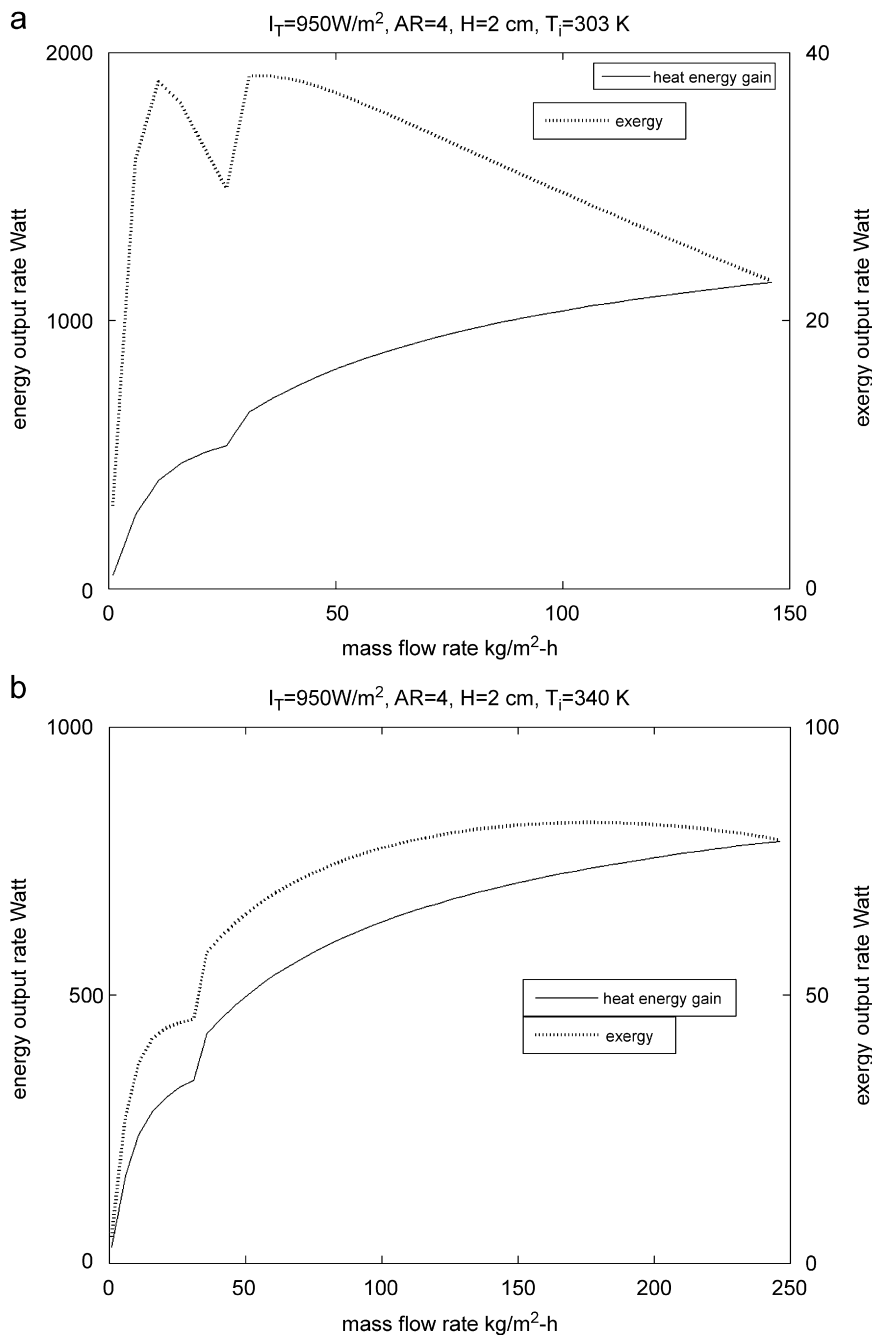


Fig. 3. Variation of exergy output rate and heat gain rate with mass flow rate, for solar radiation intensity  $950 \text{ W/m}^2$ , for (a) low and (b) high inlet temperature of air.

- Case-II: if  $T_i = (T_a + \sqrt{T_a T_{st}})/2$  then

$$m_{opt} = A_c F' U_l (T_{st} - \sqrt{T_a T_{st}}) / 2c_p \left( \sqrt{T_a T_{st}} - \frac{T_a + \sqrt{T_a T_{st}}}{2} \right)$$

$$= A_c F' U_l \sqrt{T_{st}} / c_p \sqrt{T_a}$$

From the above relation we can say that  $m$  must be finite and is about twice that of the previous case.

- Case III: if  $T_i \rightarrow \sqrt{T_a T_{st}}$  then the  $m_{opt}$  tends to infinity
- Case IV: if  $T_i \rightarrow T_{st}$  then the  $m_{opt}$  tends to zero. As for this case

$$m_{opt} = A_c F' U_l (T_{st} - \sqrt{T_a T_{st}}) / 2c_p (\sqrt{T_a T_{st}} - T_{st}) = -A_c F' U_l / 2c_p$$

Thus  $m_{opt}$  becomes negative or at such high inlet temperature there is no more positive exergy gain with flow, i.e. the flow rate should be zero.

It is evident that  $m_{opt}$  first increases with inlet temperature and then decreases. It can also be proved that the maximum exergy output for a solar intensity is achieved for an inlet temperature higher than ambient temperature. By substituting the  $(T_o + T_i)_{opt} = 2\sqrt{T_a T_{st}}$  in Eq. (22) and solving, the optimum exergy output obtained is  $(Ex_u)_{opt} = Q_u [1 - (1 - \sqrt{(T_a/T_{st})})]$  and from this relation it can be concluded that for optimum exergy output  $(Ex_u)_{opt}$  the heat energy gain or mass flow rate must be very high and thus the inlet temperature must be the geometric mean of ambient and stagnation temperature. The  $(Ex_{u,p})_{opt}$  will be at inlet temperature lower than  $\sqrt{T_a T_{st}}$  as the pump work (Eqs. (16), (20))

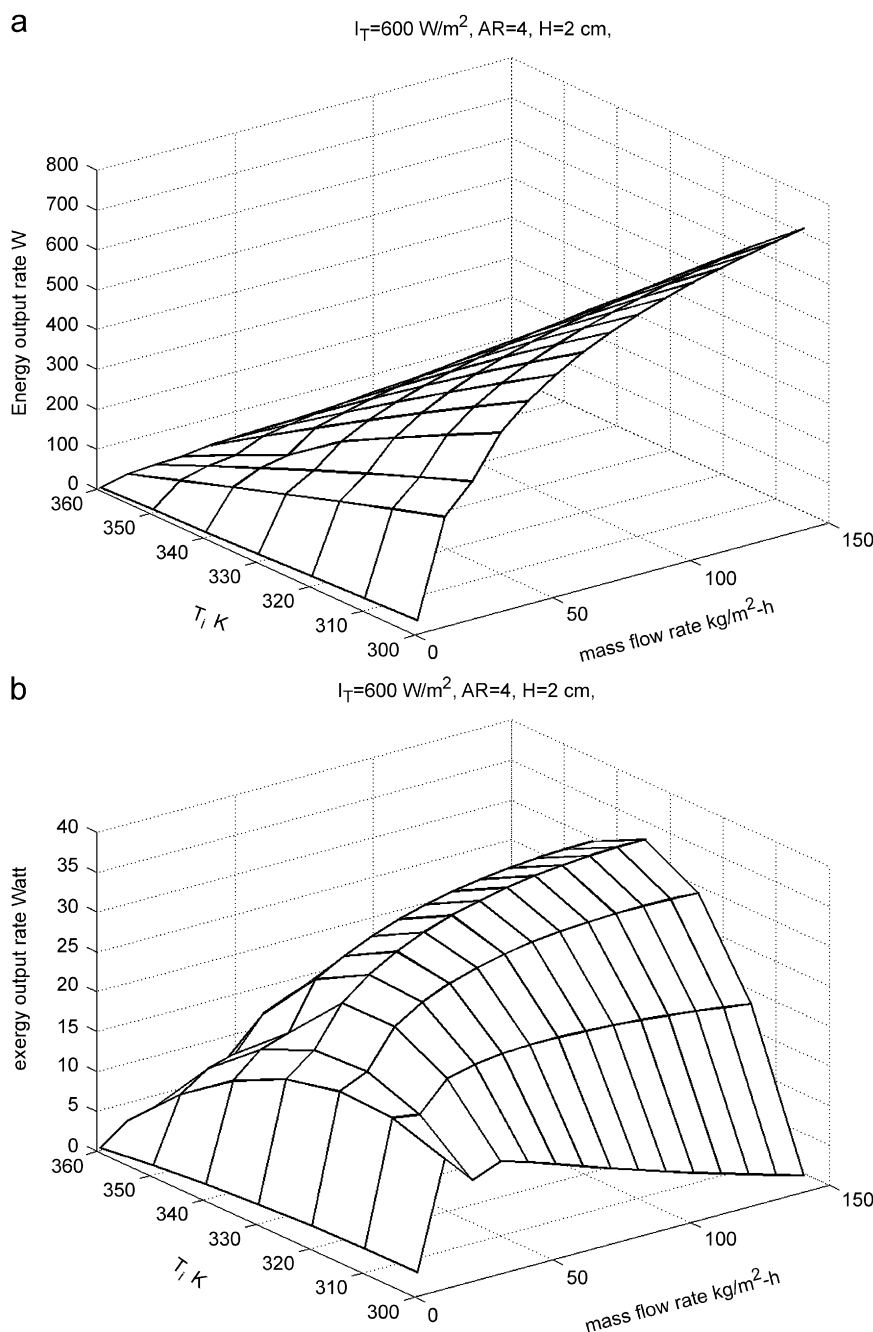


Fig. 4. Variation of (a) exergy output rate and (b) heat gain rate, with mass flow rate and inlet temperature of air, for a solar radiation intensity of 600 W/m<sup>2</sup>.

becomes significant at a higher mass flow rate. As for a solar air heater, the inlet temperature is generally equal to ambient temperature; thus for maximum exergy output, the mass flow rate must be low, but if the inlet temperature is high (may be for collectors in series) then the mass flow rate may be kept high. The solar absorbed flux or  $T_{st}$  varies throughout the day, thus for optimum exergy output the mass flow rate should be controlled accordingly, as it is unpractical to control the inlet temperature.

3. Numerical calculations

For a collector configuration, system properties and operating conditions numerical calculations have been carried out to evaluate the energy/exergy output rate of a solar air heater, for various values of collector aspect ratio (AR) of the collector, mass flow rate per unit area of the collector plate ( $G$ ) and solar air heater duct depth ( $H$ ). The air heater length and width are calculated by  $L_1 = (A_c \times AR)^{0.5}$  and  $L_2 = A_c/L_1$ , respectively, where AR is the aspect ratio of the collector. In order to obtain the results

numerically, codes have been developed in Matlab-7 using the following fixed parameters, unless otherwise mentioned:

$$A_c = 2 \text{ m}^2, K_i = 0.05 \text{ W/mK}, L = 4 \text{ cm}, \delta_b = 6 \text{ cm}, \delta_s = 4 \text{ cm}, \epsilon_p = 0.95, \epsilon_c = 0.88, \epsilon_b = 0.95, \alpha_p = 0.95, \tau_g = 0.88, \beta = 30^\circ, T_i = 30^\circ\text{C}, T_a = 30^\circ\text{C}, V_\infty = 2.5 \text{ m/s}, I_T = 600 \text{ and } 950 \text{ W/m}^2, H = 1\text{--}8 \text{ cm}, AR = 0.2\text{--}50 \text{ and } G = 0\text{--}250 \text{ kg/h-m}^2.$$

In order to evaluate the energy/exergy output rate of the collector, first initial values of  $T_{pm}$  and  $T_m$  are assumed according to the inlet temperature of air and various heat-transfer coefficients are calculated using Eqs. (9)–(15), and at temporary value of useful heat gain is estimated from Eqs. (3)–(6). The new values of  $T_{pm}$  and  $T_m$  are calculated using Eqs. (7) and (8). If the calculated new values of  $T_{pm}$  and  $T_m$  are different from the previously assumed value, then the iteration is continued with the new values till the absolute differences of the new value and the previous value of mean plate temperature as well as mean fluid temperature are less than or equal to 0.05. Air properties are determined at  $T_m$  by interpolation from air properties [25] given in Table 1. Finally calculated values of  $T_{pm}$  and  $T_m$  are used to evaluate the energy/exergy output rate using Eqs. (16), (17), (19)

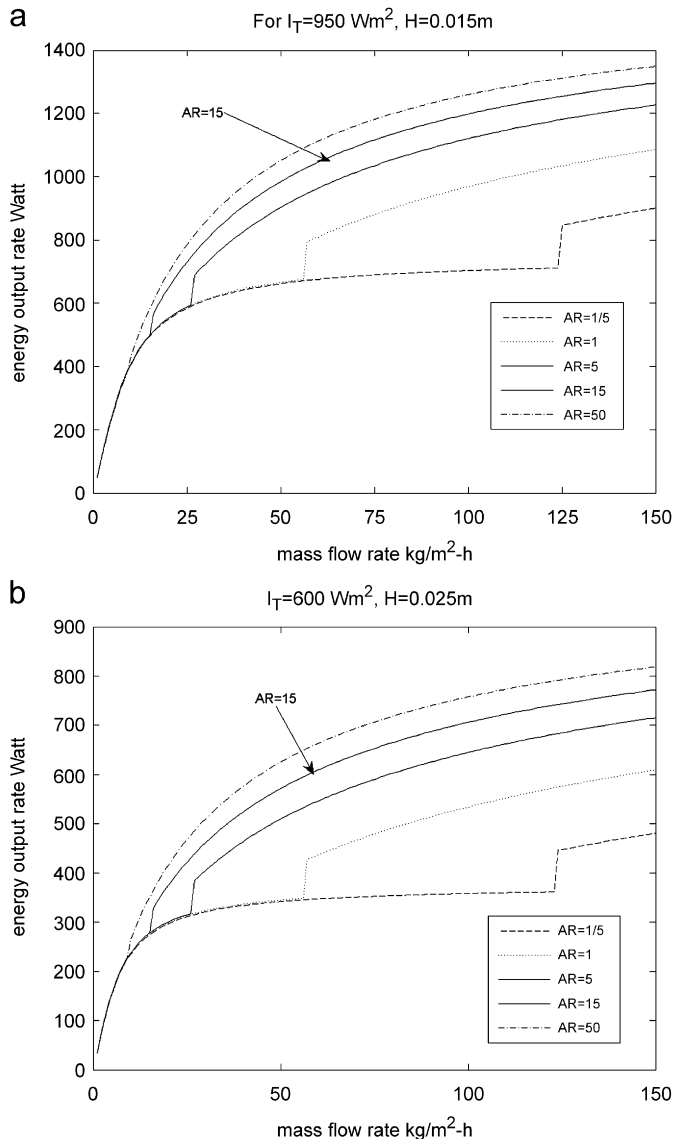


Fig. 5. Variation of heat energy output rate with mass flow rate, for various values of AR, for (a) solar radiation intensity 950 W/m<sup>2</sup> and 1.5 cm duct depth, and (b) solar radiation intensity 600 W/m<sup>2</sup> and 2.5 cm duct depth.

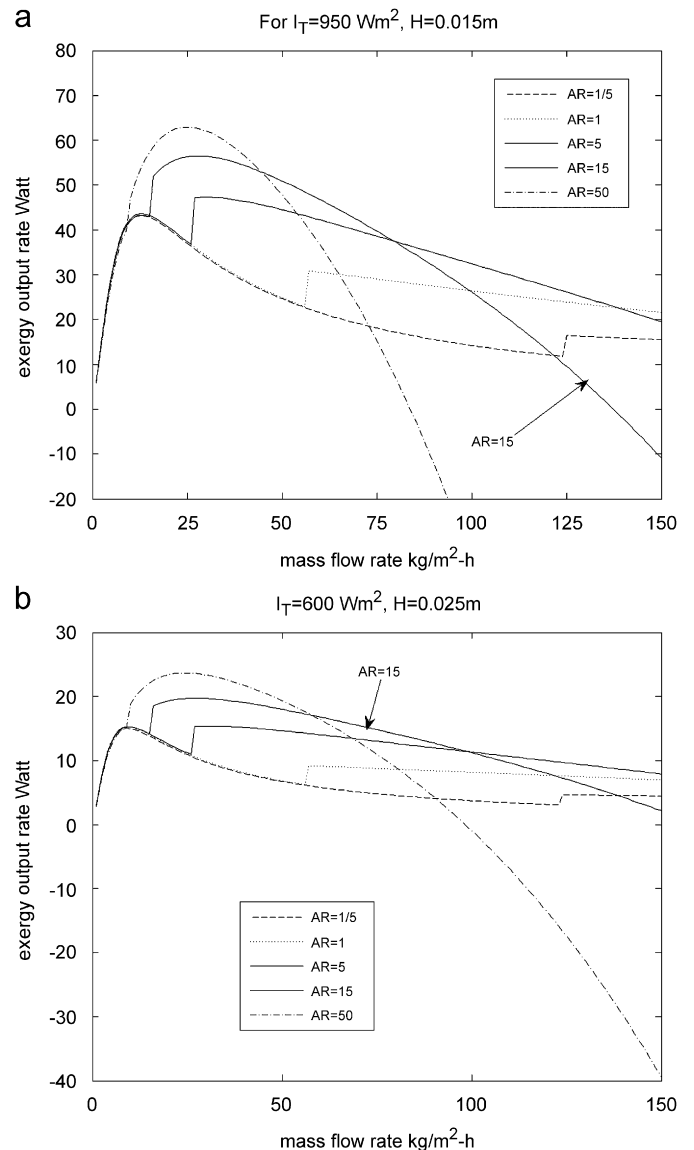


Fig. 6. Variation of exergy output rate with mass flow rate, for various values of AR, for (a) solar radiation intensity 950 W/m<sup>2</sup> and 1.5 cm duct depth, and (b) solar radiation intensity 600 W/m<sup>2</sup> and 2.5 cm duct depth.



and (20). It has been reported [1] that theoretical predictions for energy output rate/thermal efficiency agree reasonably well with the experimental results.

By sensitivity analysis it has been found that differences from the values of top heat loss coefficient, heat-transfer coefficient due to convection and coefficient of friction in the order of  $\pm 5\%$  have only small effects on the trend of variation of energy as well as exergy output rate. Sensitivity analysis shows that maximum 5% uncertainty in top heat loss coefficient changes the energy output rate in the range of 0.98–3.9% and exergy output rate by 2.5–6%; the larger variations are with very small flow rates. The energy output rate and exergy output rate change up to 1.7% and 3%, respectively, with 5% change in the value of heat-transfer coefficient due to convection, given by the used correlations. The uncertainty in the determination of coefficient of friction has no effect on the energy output rate, while the exergy output changes up to 1.5% and 4.75%, for 5% and 15% change in the value of coefficient of friction; the higher variations occur at large mass flow rates.

4. Results and discussion

4.1. Variations of useful heat energy gain, product of ambient temperature and sum of entropy created due to heating of air and pressure drop ( $T_a \times S_g$ ); energy and exergy output rate with mass flow rate and inlet temperature of air

The variations of heat energy gain and  $T_a \times S_g$  with mass flow rate are plotted in Fig. 2(a) and (b), for low and high inlet temperature of air, respectively, for a fixed values of solar radiation intensity, collector aspect ratio and duct depth. The numerical values of both terms are high for low inlet temperature and low for high inlet temperature of air. It is also clear from Fig. 2 that the heat gain increases with mass flow rate and decreases with the inlet temperature of fluid; but the difference of heat energy gain and  $T_a \times S_g$ , which is exergy output, does not follow this trend. For low inlet temperature the rate of increase of entropy created term ( $T_a \times S_g$ ) is more than the rate of increase in heat gain rate after a certain mass flow rate, and thus there is an optimum mass flow rate at low value, as proved theoretically earlier by ignoring pump work. If the temperature is high then the

rates of increase of both terms are almost same but the magnitude of heat gain is more than the entropy created term ( $T_a \times S_g$ ) up to very high mass flow rates; thus the exergy output increases with mass flow rate up to very high values of mass flow rate. The variations of exergy output rate and heat gain rate with mass flow rate are shown in Fig. 3(a) and (b), for the inlet temperatures equal to 303 and 340K, respectively, for the same values of solar intensity, collector aspect ratio and duct depth. For low inlet temperature the exergy output rate first increases, attains its maximum value and after that it decreases with mass flow rate in the laminar flow regime; the exergy output rate also decreases in the turbulent flow regime but at flow transition there is an increase in the exergy output rate due to the different correlations of heat-transfer coefficient and friction factor for laminar and turbulent flow. For high inlet temperature, the exergy output rate increases continuously up to some mass flow rate in turbulent flow, though the rate of change of exergy output rate decreases with the value of mass flow rate; and at very high flow rate, the exergy output will become zero due to increased pressure drop. Fig. 3 and mathematical relations 2, 3 and 19 indicate that there should be a global optimum inlet temperature for a particular

Table 2 Optimum G, corresponding energy output, exergy output and flow Reynolds number with AR for  $H = 1.5$  cm,  $I_T = 950$  W/m<sup>2</sup> and  $T_i = 303$  K

AR	Optimum G	Q	Ex	Re
0.2	13	466.0852	43.23936	221.8242
1	13	468.5899	43.67184	492.8941
2	13	468.7899	43.70355	693.9912
3	13	468.6893	43.68293	847.1406
4	30	708.6332	45.21006	2336.569
5	30	725.6473	47.28312	2601.806
10	29	761.7861	53.35423	3502.644
20	27	775.3353	58.52768	4518.592
30	26	780.3624	60.9102	5255.067
40	26	792.6068	62.21167	6008.319
50	25	785.4247	62.94462	6393.256
60	24	775.0713	63.32309	6660.515
70	24	779.7543	63.49043	7145.999
80	23	765.9108	63.48638	7261.143
90	23	768.8312	63.37833	7657.821
100	22	752.6554	63.16884	7663.225
110	22	754.5705	62.91454	7997.064
120	22	756.1755	62.58441	8313.159
130	21	737.8237	62.23795	8203.025
140	21	738.902	61.85049	8476.142
150	21	739.8142	61.41543	8737.594

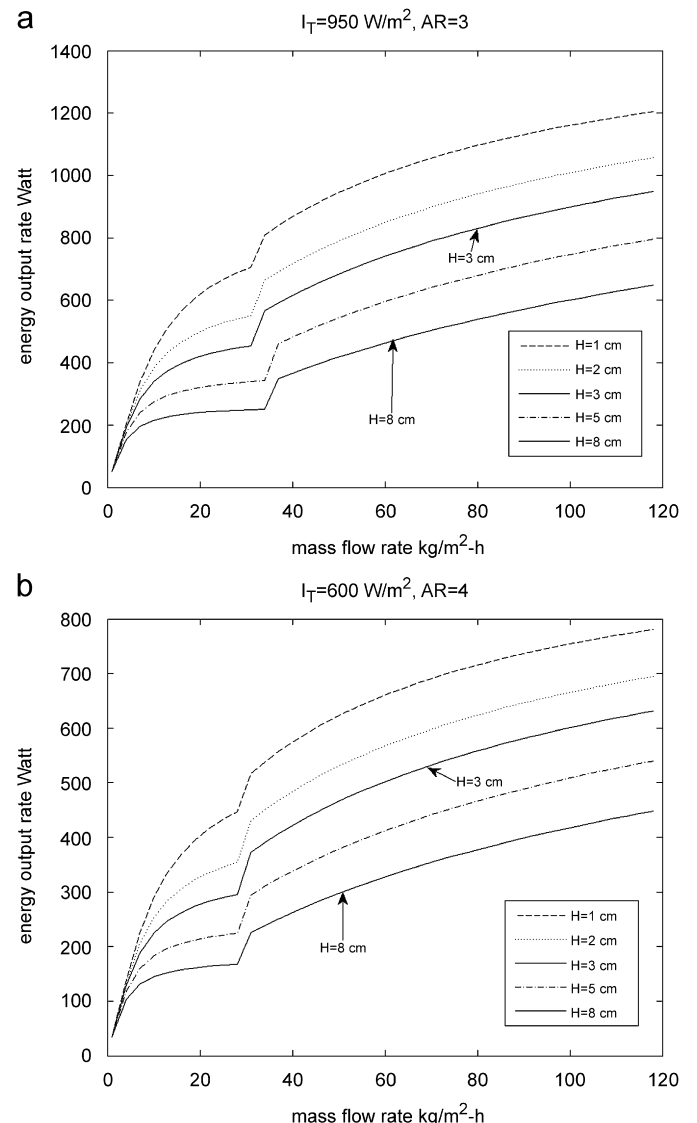


Fig. 7. Variation of exergy output rate with mass flow rate, for various values of H, for (a) solar radiation intensity 950 W/m<sup>2</sup> and AR = 3, and (b) solar radiation intensity 600 W/m<sup>2</sup> and AR = 4.

solar intensity. It can be observed from Fig. 3 that the maximum exergy output for low inlet temperature is less than 40W while for high it is more than 80W, and for very high value of inlet temperature the heat gain and thus exergy output may become negative. Using Eqs. (2) and (3) the  $T_o$  from Eq. (19) can be eliminated. The resulting equation for exergy output is a function of inlet temperature and other parameters. If other parameters ( $F_r, U_l$ ) are treated constant then there should be an optimum  $T_i$  for a particular  $m$  and  $l$ . The variations of energy output or heat gain rate, and exergy output rate, with mass flow rate and inlet temperature, are shown in Fig. 4(a) and (b), respectively. The values of collector aspect ratio and duct depth are taken to be the same while the solar radiation intensity is different. It is evident from Fig. 4(a) that heat gain rate increases with mass flow rate, and decreases with inlet temperature. It is clear from Fig. 4(b) that there is a global optimum inlet temperature that maximizes the exergy output for a given value of solar radiation intensity. The increase in exergy output (Fig. 4) with mass flow rate for any  $T_i$  is not significant after a certain value of mass flow rate in the low

range. It can be concluded from Figs. 3 and 4 that both energy as well as exergy output rate decrease as the solar intensity reduces.

4.2. Variations of useful heat energy and exergy output rates for various aspect ratios of the solar collector with mass flow rate

The energy and exergy output rates were evaluated for various values of collector aspect ratio (AR) and mass flow rate per unit area of the collector plate ( $G$ ). The inlet temperature of air is taken equal to ambient temperature. Fig. 5(a) and (b) shows the improvement in energy output rate with AR and  $G$  as pointed by other investigators. The increase in energy output rate with  $G$  is more for a higher value of AR. It is evident from Fig. 5 that the energy output rate increases as AR increases. The enhancement in the energy output rate is due to the fact that increase in AR or  $G$  results in increased velocity of flow due to the reduction of cross-sectional area of the collector duct or increase in mass flow rate, accompanied with enhanced convective heat-transfer coefficient

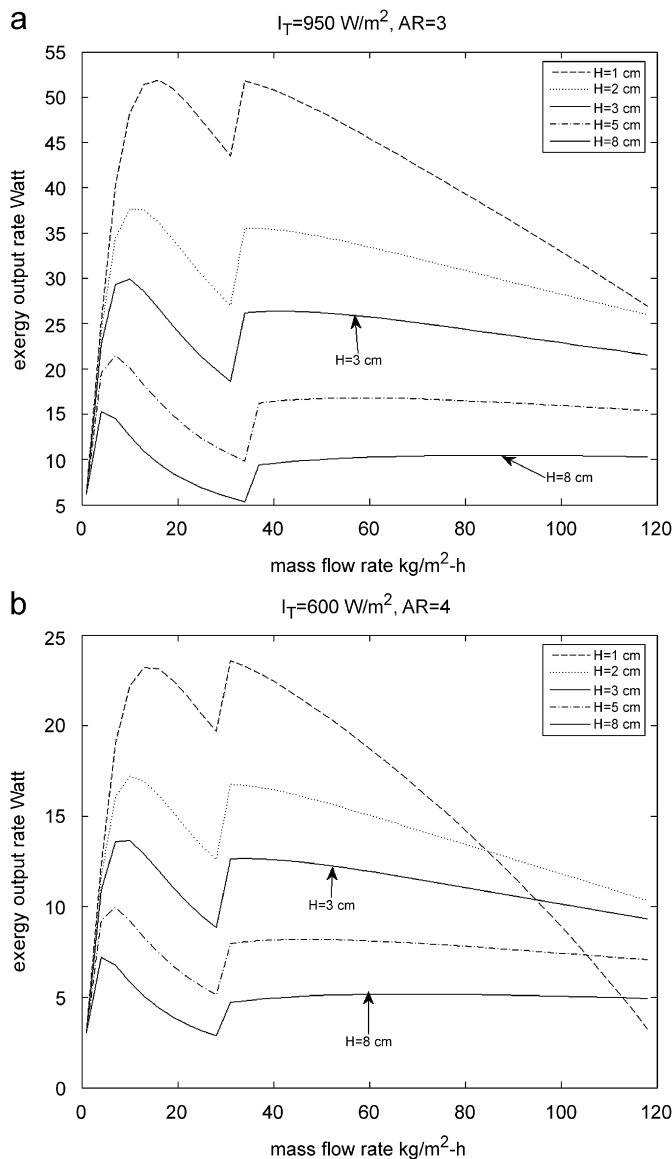


Fig. 8. Variation of exergy output rate with mass flow rate, for various values of  $H$ , for (a) solar radiation intensity  $950\text{ W/m}^2$  and  $AR = 3$ , and (b) solar radiation intensity  $600\text{ W/m}^2$  and  $AR = 4$ .

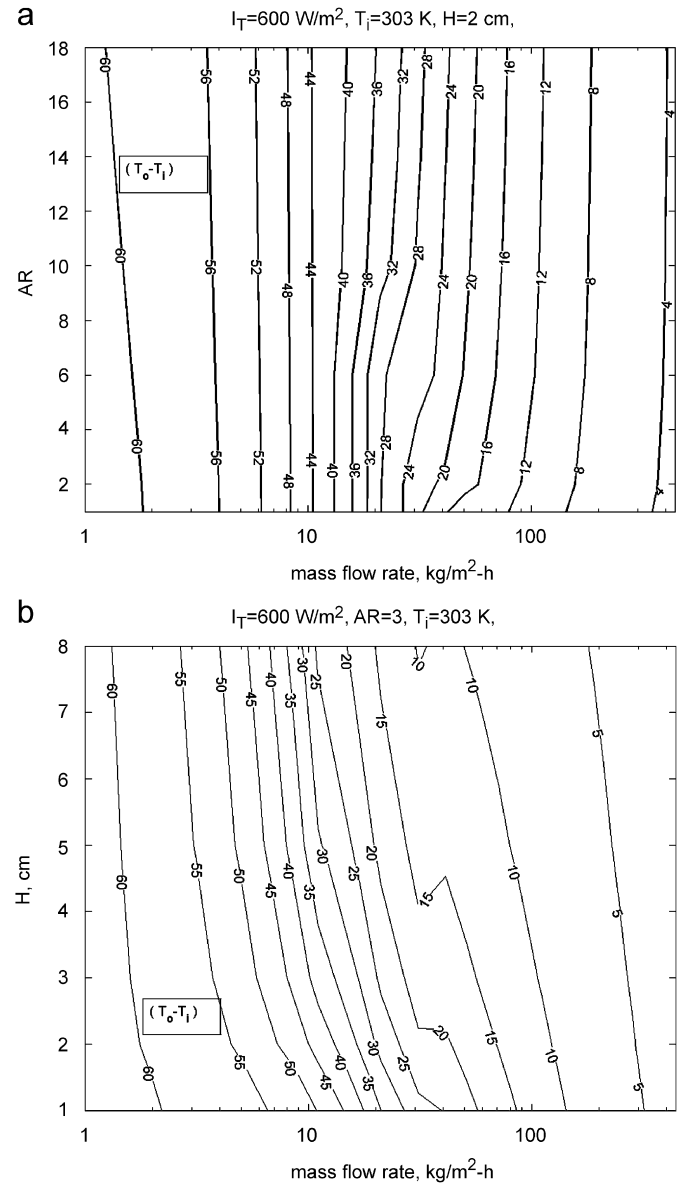


Fig. 9. Variation of temperature increase of air with mass flow rate (a) for various values of AR and (b) for various values of  $H$ .

through the duct. It can be concluded that for better energetic performance the  $G$  and  $AR$  must be high. However, the energetic analysis view point completely ignores the pump/blower work requirement and quality of heat energy collected. Fig. 6(a) and (b) shows the variation of exergy output rate with  $AR$  and  $G$ , and it is evident from this figure that the exergy output rate does not increase monotonically with  $G$  (as proved earlier for a low inlet temperature of air), and  $AR$ . For low mass flow rate, the exergy output rate increases with  $AR$  up to larger values of  $AR$ . Thus higher  $AR$  may be used to gain optimum exergy output for a low inlet temperature of air. It is clear from Fig. 6 that for higher values of  $G$ , the exergy output rate decreases with  $G$  and  $AR$ . This rate of decrease of exergy output with higher  $G$  increases with  $AR$ . Thus, for maximum exergy output, the  $AR$  should not be more if  $G$  is high. It can be understood from Fig. 6 that the optimum

$G$  depends on  $AR$ ; thus the variations of optimum  $G$  and corresponding energy output, exergy output and flow Reynolds number with  $AR$  are given in Table 2. It can be seen from Table 2 that as  $AR$  increases, the optimum  $G$  first increases due to transition or turbulent flow and then decreases; for higher  $AR$  the optimum exergy output also decreases.

#### 4.3. Variations of useful heat energy and exergy output rate for various duct depths of the solar collector with mass flow rate

Figs. 7(a) and (b), and 8(a) and (b) show the variation of energy and exergy output rates, respectively, with mass flow rate per unit area of the collector plate ( $G$ ) for various values of duct depth ( $H$ ). The inlet temperature of air is taken equal to ambient

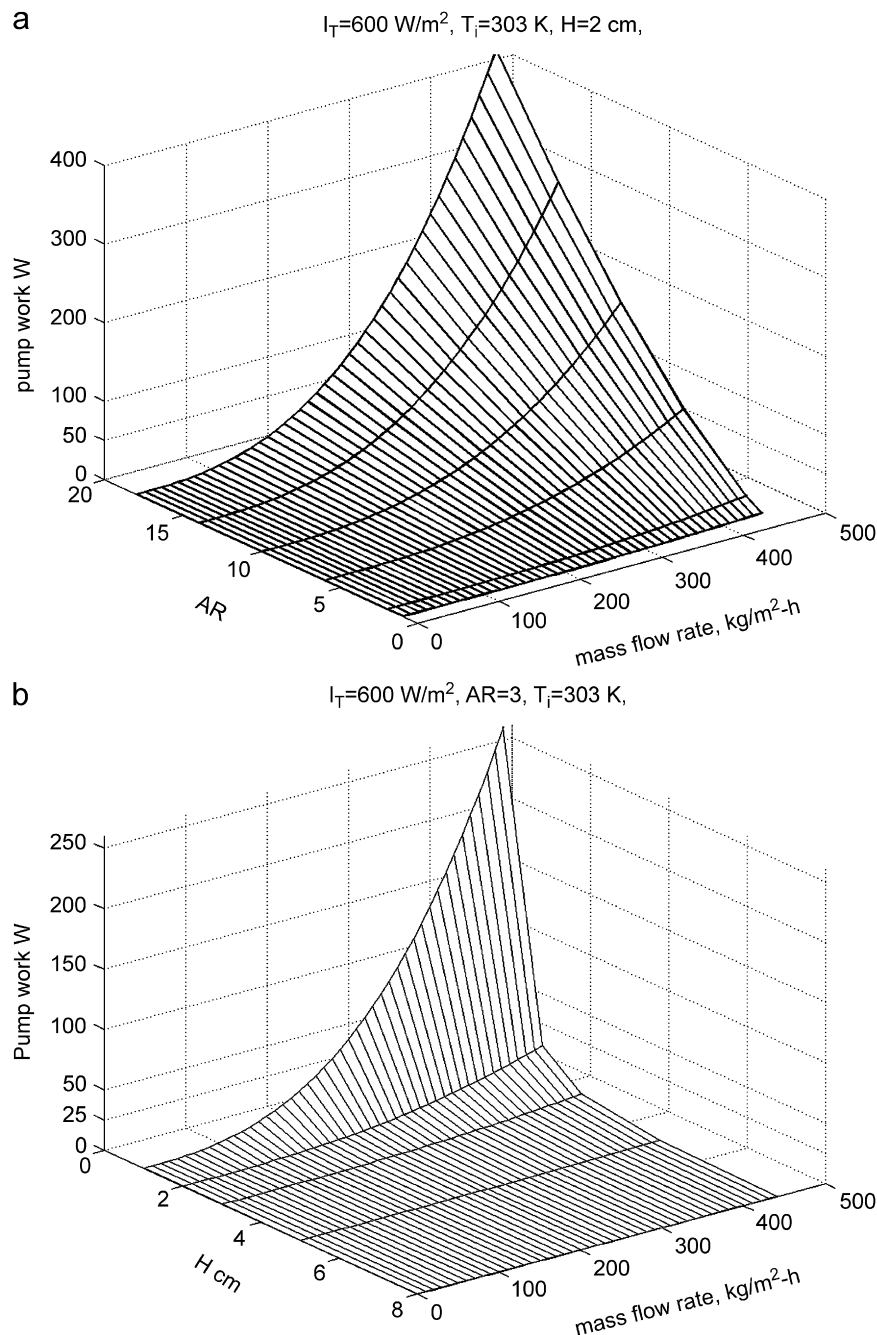


Fig. 10. Variation of pump work with mass flow rate of air (a) for various values of  $AR$  and (b) for various values of  $H$ .

temperature. It is evident from Fig. 7 that the energy output rate is high at lower values of duct depth, regardless of the other parameters, and for higher energetic performance the duct depth should be low. The exergy output rate does not show monotonous trend (Fig. 8) with decrease in duct depth; it depends on AR and  $G$ . At low  $G$  the exergy output rate is also high for lesser duct depth, but it decreases at a faster rate with  $G$  for low duct depth. Thus, for the maximum exergy output the  $H$  should be low only if  $G$  is low.

#### 4.4. Variations of temperature rise of air and pump work with $G$ , AR and $H$ : importance of exergy

Fig. 9(a) shows the variation of temperature increase of air with  $G$  and AR, while Fig. 9(b) shows the variation of temperature increase of air with  $G$  and  $H$ . As high temperature increase is more useful as per utility view point, it can be said that  $G$  must be very low. But at very low value of  $G$  the useful heat gain will also be very small. The temperature rise for a given flow rate changes more with  $H$  in comparison to AR; it may be said that AR must be very high and  $H$  must be low. The variation of required pump work with  $G$  and AR is shown in Fig. 10(a), while Fig. 10(b) shows the variation with  $G$  and  $H$ . It is evident that the required pump work increases with increase in  $G$  and AR, and decrease in  $H$  as per the power law. It is also clear from Fig. 10 that for extreme values of  $G$ , AR and  $H$ , the required pump work becomes quite high. It even exceeds the maximum exergy output, ignoring the pressure drop that can be obtained for the given solar radiation intensity. The temperature rise criterion alone recommends the use of very low  $H$  and  $G$ ; but in order to get significant energy output the  $G$  must be finite. The energy output criterion recommends using high AR and  $G$ , and low  $H$ . For higher values of  $G$ , not only the temperature rise of air or usefulness reduces, but the pump work may also become significant.

Thus to incorporate the quality of heat energy collected and required pump work, the second law-based exergy is a suitable quantity. The energy-based criteria do not give the optimum values of  $G$ , AR and  $H$ ; hence optimal performance parameters, for particular application of SAH, should be decided using the exergy output.

## 5. Conclusion

It can be said that as per the energy output rate evaluation criterion the solar air heater should have high AR and  $G$ , and low duct depth and low inlet temperature of air. The exergy output depends on heat gain and entropy created term; thus it incorporates the temperature rise of air and pump work. It has been proved and observed that if the inlet temperature of air is low than maximum exergy output is achieved at low value of mass flow rate but if inlet temperature of fluid is high then exergy output increases with mass flow rate though gain at very high mass flow rate is not significant. It has also been deduced that for optimum exergy output ignoring the pressure drop the optimum inlet temperature is geometric mean of ambient and stagnation temperature, while for optimum exergy output considering the

pressure drop, the optimum inlet temperature is lesser than this geometric mean and more than ambient. For air heater applications, the inlet temperature is generally ambient and may be more for collectors in series; a slight high flow rate may be kept for the latter case. The exergy output rate evaluation criterion shows that there will be optimum values of AR and  $H$ ; and optimum depends on  $G$  to suit a particular application. As air heater applications are governed by temperature rise required or mass flow rate, the decision should be made by requirement of application. In the case of air heater, the required pump work increases rapidly with  $G$ ; thus if  $G$  is low then high AR and low  $H$  will give higher exergy output, while for higher  $G$  the reverse is true.

## References

- [1] Yeh HM, Lin TT. The effect of collector aspect ratio on the energy collection efficiency of flat-plate solar air heaters. *Energy* 1995;20:1041–7.
- [2] Yeh HM, Lin TT. Efficiency improvement of flat-plate solar air heaters. *Energy* 1996;21:435–43.
- [3] Yeh HM, Lin TT. Solar air heaters with two collectors in series. *Energy* 1997;22:933–6.
- [4] Karwa R, Garg SN, Arya AK. Thermo-hydraulic performance of a solar air heater with n-sub-collectors in series and parallel configuration. *Energy* 2002;27:807–12.
- [5] Kotas TJ. The exergy method of thermal plant analysis. Butterworths; 1985.
- [6] Bejan A. Advanced engineering thermodynamics. Wiley Interscience Pub; 1988.
- [7] Kaushik SC, Mishra RD, Singh N. Second law analysis of a solar thermal power system. *Int J Sol Energy* 2000;20:239–53.
- [8] Lior N, Sarmiento-Darkin W, Al-Sharqawi Hassan S. The exergy fields in transport processes: their calculation and use. *Energy* 2006;31:553–78.
- [9] Rosen MA, Dincer I. A study of industrial steam process heating through exergy analysis. *Int J Energy Res* 2004;28:917–30.
- [10] Kanoglu M, Dincer I, Rosen MA. Understanding energy and exergy efficiencies for improved energy management in power plants. *Energy Policy* 2007;35:3967–78.
- [11] Lior N, Zhang N. Energy, exergy, and Second Law performance criteria. *Energy* 2007;32:281–96.
- [12] Howell JR, Bannerot RB. Optimum solar collector operation for maximizing cycle work output. *Sol Energy* 1977;19:149–53.
- [13] Bejan A. Extraction of exergy from solar collectors under time-varying conditions. *Int J Heat Fluid Flow* 1982;3:67–72.
- [14] Bejan A. Entropy generation through heat and fluid flow. New York: Wiley-Interscience; 1982.
- [15] Manfrida G. The choice of an optimal working point for solar collectors. *Sol Energy* 1985;34:513–5.
- [16] Kar AK. Exergy efficiency and optimum operation of solar collectors. *Appl Energy* 1985;21:301–14.
- [17] Suzuki A. General theory of exergy-balance analysis and application to solar collectors. *Energy* 1988;13:153–60.
- [18] Altfeld K, Leiner W, Fiebig M. Second law optimization of flat-plate solar air heaters part I: the concept of net exergy flow and the modeling of solar air heaters. *Sol Energy* 1988;41:127–32.
- [19] Altfeld K, Leiner W, Fiebig M. Second law optimization of flat-plate solar air heaters. Part 2: Results of optimization and analysis of sensibility to variations of operating conditions. *Sol Energy* 1988;41:309–17.
- [20] Torres-Reyes E, Cervantes-de Gortari JG, Ibarra-Salazar BA, Picon-Nunez M. A design method of flat-plate solar collectors based on minimum entropy generation. *Exergy Int J* 2001;1:46–52.
- [21] Luminosu I, Fara L. Determination of the optimal operation mode of a flat solar collector by exergetic analysis and numerical simulation. *Energy* 2005;30:731–47.
- [22] Malhotra A, Garg HP, Palit A. Heat loss calculation of flat plate solar collectors. *J Therm Energy* 1981;2:2.
- [23] Kays WM. Convective heat and mass transfer. New York: McGraw-Hill; 1966.
- [24] Duffie JA, Beckman WA. Solar engineering of thermal processes. New York: Wiley; 1991.
- [25] Sukhatme SP. Solar energy: principles of thermal collection and storage. New Delhi: Tata McGraw-Hill; 1987.